Effect of MoS2 layer on the LSPR in periodic nanostructures

Mohamed El Barghouti, Abdellatif Akjouj, Abdellah Mir

HAL Id: hal-03183504

https://hal.science/hal-03183504

Submitted on 20 Aug 2021

Effect of MoS$_2$ layer on the LSPR in periodic nanostructures

Mohamed El Barghouti[a,*], Abdellatif Akjouj[b], Abdellah Mir[a]

[a] *Laboratory for the Study of Advanced Materials and Applications (LEM2A), Physics Department, Faculty of Science, Moulay Ismail University, B.P. 11201, Zitoune, Mekns, Morocco*
[b] *Institute of Electronics, Microelectronics and Nanotechnology, UMR CNRS 8520, Lille University, FST, Department of Physics, 59655 Villeneuve dAscq, France*

In this work, we propose a new configuration of the localized surface plasmon resonance (LSPR), based on MoS$_2$ hybrid structures for ultrasensitive biosensing applications. The plasmonic resonances are widely used in bimolecular detection and continue to be an active network because of the rich variety of surface configurations and measurement donations. The present work studies the interaction of gold nanoparticles with a MoS$_2$ film. MoS$_2$ is used as a thin spacer between the gold nanoparticles and the dielectric medium used for detection. MoS$_2$ monolayers have emerged recently as promising nanostructures for various applications in both the optics and electronics. This paper gives an overview of the optical properties of 2D nanostructures based on this new class of materials. A stronger behavior of the resonance positions in the absorption spectrum exhibits a strong coupling between the LSPR on the gold nanoparticles and the MoS$_2$ coating film. Numerical simulations display a significant red shift of the plasmonic resonance (λ_{max}) and the results show that using a 3.90 nm MoS$_2$ layer, the plasmon resonance wavelength is increased of 333.7 nm. We also study the performance of the proposed biosensors in terms of sensitivity using multilayers of MoS$_2$ and normal incidence to the surface of SiO$_x$/AuNPs/MoS$_2$/ water and SiO$_x$/MoS$_2$/AuNPs/water. We obtain a very high sensitivity of 297.62 nm/RIU corresponding to an increase of 26% compared to the results obtained on SiO$_x$/AuNPs/water, with a location of the electric field on the gold nanoparticles and the covering MoS$_2$ layer. These characteristics should make these biosensors a preferred choice for detection applications.
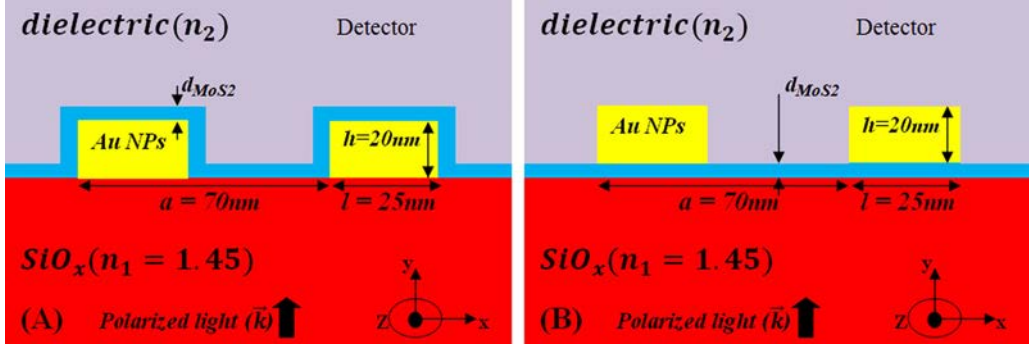
1. Introduction

Plasmonic response of the metal nanoparticles is highly dependent on their size [1–3], their form [4–6] and the material constituting the chemical 2D composition [7–9]. The understanding of their properties is even more complex when they are deposited on a substrate [1,10,11] or when they interact with each other [12–14]. It appears from the theoretical and the experimental studies already completed that there are many parameters governing their behavior [15]. As part of our study, we will investigate the influence of the MoS$_2$ layer on the LSPR. The complex refractive index of the MoS$_2$ monolayer obtained from the experimental measurement data by Castellanos-Gomez et al. [16] is $n_{\mathrm{MoS_2}} = 5.9 + 0.8i$ at 632.8 nm and the thickness of the MoS$_2$ layer is $d_{\mathrm{MoS_2}} = N \times 0.65$ nm [17,18], where N is the number of coatings of MoS$_2$ [19–22], deposited on the metal nanoparticles of gold. Molybdenum disulfide (MoS$_2$) holds great promise for optical applications due to the variations of optical transition depending on the atomic thickness of the film [19]. A gradual red shift of the absorption bands the background absorption. Hence, Increasing MoS$_2$ film thickness is observed to allow tuning the absorption properties of such films. The optical processes in a low dimensional materials

---

* Corresponding author.
 E-mail address: Mohamedaziz1989@hotmail.fr (M.E. Barghouti).

Fig. 1. Schematic representation of the plasmonic structures studied in this work. (A) Periodic gold nanoparticle (Au NPs) array on SiO_x ($n_1 = 1.45$) and coated with a layer of MoS_2 (SiO_x/AuNPs/MoS_2); (B) SiO_x ($n_1 = 1.45$) coated with a thin film of MoS_2 onto which a periodic gold nanoparticle (Au NPs) was deposited (SiO_x/MoS_2/Au NPs). The height ($h = 20$ nm), width ($l = 25$)) and lattice parameter ($a = 70$ nm) defined as the closest distance between two adjacent AuNPs is the same in both cases. The input source is placed in the substrate (SiO_x) and the detector in the dielectric, being water ($n_2 = 1.333$).

such as MoS_2 can furthermore be changed by the presence of resonance cavities and plasmonic nanostructures [16]. In biosensing applications, the gold is not well adapted because of its poor absorption of biomolecules, causing limitations on the sensitivity of the biosensor [23]. As a solution to this limitations, the gold layer is substituted for the gold nanoparticles (AuNPs). Gold nanoparticles have a unique property called localized surface plasmon (LSPR). The AuNPs-based LSPR is widely used for the detection [24]. In addition, the dielectric environment of the Localized surface plasmons resonance (LSPR) has been extensively studied in recent years [25,26] 2D networks nanoparticles of gold (AuNPs). In this work, we theoretically study the impact of the MoS_2 substrate thickness on the plasmonic signal of gold nanoparticle (AuNPs) arrays (Fig. 1B). Throughout this paper, the geometrical parameters of the AuNPs is fixed with l is the particles length, a is the lattice parameter (along x-axis), and h is the particles height. It is well established that AuNPs strongly absorb within narrow frequency bands in the visible range as their localized surface plasmon resonances get excited. Besides, the effect of the dielectric environment surrounding the AuNPs has been widely studied [27,28]. A part of this work consists of investigating numerically the influence of MoS_2 coatings (0–7.15 nm) on the localized surface plasmon resonance signal of AuNPs arrays (Fig. 1A). In the first part, the idea is to highlight the role of a few layers of MoS_2 as one of the finest collection thickness of layers deposited on MoS_2 nanostructures. The considered ranging is from 0 nm to 3.90 nm (strong red shift of the resonance). The layers of the dielectric have been deposited on a substrate of SiO_x ($n_1 = 1.45$) over which two types of nanostructures have been investigated. In the second part, numerical simulations of structures SiO_x/AuNPs/MoS_2/water and SiO_x/MoS_2/AuNPs/water with a normal bias following the z-axis, show significant sensitivity ~ 300 (nm RIU^{-1}) Fig. 1(A) and ~ 171 (nm RIU^{-1}) Fig. 1(B) for the eight layers MoS_2 5.20 nm [29–34]. In addition, the plasmonic response of metal nanoparticles with various geometrical parameters gold nanoparticles $l = 125$ nm, $a = 300$ nm, and $h = 15$ nm. These results are consistent with other reports in the literature showing long row detecting refractive index on plasmonic nanostructures [15,20,22]. The distributions of the electric field structures excited to resonance at normal incidence and represented by the maps of the 2D and 3D electrical fields which indicate that this mode is a localized surface plasmon dipole whose hot spots (areas of high intensities field) are pushed to the top and bottom corners of AuNPs for the structure SiO_x/AuNPs/MoS_2/water, and top corners of AuNPs to layer MoS_2 under the nanoparticles to the structure SiO_x/MoS_2/AuNPs/water to the lengths wave resonances (λ_{max}).

One observes a significant enhancement of the sensitivity of localized surface plasmon resonances of coated AuNPs with layers of MoS_2 to the surrounding environment as compared to bare nanoparticles. Hence, the design of Au nanoparticles/MoS_2 based-plasmonic bio-sensors with more sensitive could be reached. Indeed, we show that AuNPs coating with few layers of MoS_2 leads to approximately a 26% higher sensitivity. The optimal thickness of MoS_2 layers is numerically investigated to achieve a high LSPR sensitive system.

2. Theoretical methods

The optical properties of gold nanoparticles are solved numerically, in the frequency domain, using the scattered field formulation. Field analysis was performed using a commercially available Finite Elements Method (FEM) method package (COMSOL Multiphysics 4.4) [35,36]. The simulation method has been well documented [37–39]. A layer of gold nanoparticles of diameter (l), height (h) and interparticle distance (a), is coated with a MoS_2 thin-layer and immersed in a homogeneous matrix. A transparent glass of SiO_x (refractive index $n_1 = 1.45$) is used as a substrate. The frequency-dependent complex permittivity of metal (gold) is described by the Lorentz–Drude model (Eq. (1)) [40,41].

$$\varepsilon(\omega) = \varepsilon_{r,\infty} + \sum_{m=0}^{M} \frac{f_m \omega_p^2}{\omega_m^2 - \omega^2 + j\omega\Gamma_m}$$

(1)

where $\varepsilon_{r,\infty}$ is the relative permittivity at infinite frequency, ω_p the plasma frequency, and ω_m, f_m and Γ_m the resonance frequency,

Table 1
Gold (Au) Lorentz–Drude model parameters.

Term	f_m (rad/s)	ω_p (rad/s)	ω_m (rad/s)	Γ_m (rad/s)
$m = 0$	0.760	13.72×10^{15}	0.00	0.08052×10^{15}
$m = 1$	0.024	13.72×10^{15}	0.6305×10^{15}	0.3661×10^{15}
$m = 2$	0.010	13.72×10^{15}	1.261×10^{15}	0.5241×10^{15}
$m = 3$	0.071	13.72×10^{15}	4.511×10^{15}	1.322×10^{15}
$m = 4$	0.601	13.72×10^{15}	6.538×10^{15}	3.789×10^{15}
$m = 5$	4.384	13.72×10^{15}	20.24×10^{15}	3.364×10^{15}

strength and damping frequency, respectively, of mth oscillators. The Lorentz–Drude model uses M damped harmonic oscillators to describe the small resonances observed in the metals frequency response. The values of the constants in Eq. (1) are taken from reference [40], with the value of the dielectric constant of infinite frequencies being $\varepsilon_\infty = 1$. The values of the other parameters are listed in Table 1:

3. Results and discussion

3.1. Localized surface plasmon for periodic nanostructures

The evolution of the localized surface plasmon modes in 2D periodic nanostructures on two different surface architectures are investigated (Fig. 1). The morphology of the periodic gold nanoparticle such as particle diameter (l), height (h), and period (a) is kept the same. The difference between the two structures is the position of the dielectric MoS$_2$ layer, being either around the Au NPs (Fig. 1A) or below the Au NPs (Fig. 1B). A transparent glass substrate SiO$_x$ with $n_1 = 1.45$ is used in both cases and the assembly immersed in a non-absorbing medium such as water ($n_2 = 1.333$).

For the refractive index of MoS$_2$, we have used a constant value $n_{\text{MoS}_2} = 5.9 + i\,0.8$ (at 632.8 nm) [16,17], the thickness of the MoS$_2$ layer being estimated by $d_{\text{MoS}_2} = N \times 0.65$ nm, where N is the number of MoS$_2$ layers, and we have not used the function of the wavelength $n_{\text{MoS}_2} = \sqrt{\varepsilon(\omega)}$ [42], because in our nanostructures the absorption spectra either varies in the thickness of the MoS$_2$ layer or in the detection refractive index medium. This simulation demonstrates a single peak that varies and the two skins remain fixed. So, in our work we focus on the plasmon resonance of localized surface which changes according to the parameters of nanostructures. In other different computational checks we have noticed that we are using a fixed value of n_{MoS_2}.

The LSPR spectrum of a glass/AuNPs interface where the AuNPs parameters were set to a length of 25 nm, a height of 20 nm and a period of 70 nm, shows a plasmon resonance at 525 nm Fig. 2(A). As expected, an increase in the thickness of MoS$_2$ shifts the peak wavelength maximum λ_{max} to the red, from $\lambda_{max} = 538$ nm for $d_{\text{MoS}_2} = 0.65$ nm (monolayer) to $\lambda_{max} = 611$ nm for $d_{\text{MoS}_2} = 3.90$ nm (six layers). In addition, the presence of MoS$_2$ results in a considerable increase in the overall absorption intensity in the near-infrared Fig. 2(B). It also seems that some additional badly defined bands are occurring in the presence of MoS$_2$ thicknesses above 1.3 nm.

In Fig. 2B, we have plotted the evolution of the plasmon resonance wavelength in relation to the thickness of the dielectric layer MoS$_2$ calculated for interfaces SiO$_2$/AuNPs/MoS$_2$/water. Was found that an increase in the thickness of MoS$_2$ (d_{MoS_2}) shifts the peak wavelength (λ_{max}) to red almost linearly from $\lambda_{max} = 538.21$ nm for $d_{\text{MoS}_2} = 0.65$ nm up to $\lambda_{max} = 611.25$ nm for $d_{\text{MoS}_2} = 3.90$ nm, due to the interaction of AuNPs/MoS$_2$ with a normal incident light pulse.

In the case of MoS$_2$ present on the glass interface rather than the Au NPs (Fig. 1(B), the plasmonic behavior is rather different. With increasing MoS$_2$ thickness, next to a band at 525 nm, a second strongly absorbing plasmon band is observed and shifts to higher wavelength with increase of the thickness of MoS$_2$ Fig. 2(C).

For the structure SiO$_x$/MoS$_2$/AuNPs Fig. 2(C), we observe that we add the MoS$_2$ layer between the substrate and the AuNPs, the refractive index of medium under the nanoparticles increase SiO$_x$ ($n_1 = 1.45$) $< n_2$ to SiO$_x$/MoS$_2$ ($n_{\text{MoS}_2} = 5.9 + 0.8i$) $> n_2$ leads to an increase in the resonant wavelength rapidly, an enlargement of the plasmon band, as well as the appearance of a multimodal response [43]. The evolution of the amplitude of the oscillations thus seems to result from the competition between several phenomena. Two of them help to reduce the amplitude of the oscillations when n_1/n_{MoS_2} becomes larger than the detection medium refractive index. This is the decrease in the contrast of the standing wave system inside the cavity on the AuNPs, and the appearance of a second peak plasmonic response (multimodal). The last phenomenon is the increase of the spectral width of the main plasmonic mode with the increase in the thickness of the MoS$_2$ layer, which tends to increase the amplitude of surface plasmon oscillations.

The position of the resonant wavelength plasmon λ_{max} shifts almost linearly with the increase of MoS$_2$ thickness to $\lambda_{max} = 865$ nm for (d_{MoS_2}) = 3.90 nm Fig. 2(D). In contrast to glass/AuNPs/MoS$_2$, the position of to λ_{max} is unchanged for glass/MoS$_2$/AuNPs interface when changing the refractive index of the immersion medium (from $n_2 = 1$ to $n_2 = 1.45$) Fig. 3. In the case of glass/AuNPs/MoS$_2$, a shift is observed for all thicknesses of MoS$_2$.

The influence of refractive index at the interface of the structure SiO$_x$/AuNPs/MoS$_2$ was investigated by recording the wavelength shift when it is changed. In different proportions giving refractive indices ($n_2 = 1.333$ for water, 1 for air and 1.45 SiO$_x$), the response of the absorption spectrum of LSPR is generally described in Fig. 3(A). It shows that the position of λ_{max} moves the higher wavelength 530 nm (air) 542 nm (SiO$_x$) to a layer of MoS$_2$ (0.65 nm) while increasing the refractive index of the detection medium [44,45]. For the SiO$_x$/MoS$_2$/AuNPs structure, conservation λ_{max} has been observed for the change in refractive index ($n_2 = 1$, 1.333 and 1.45) Fig. 3(B), followed by a very large red shift of the length wave between 0.65 nm $\leq d_{\text{MoS}_2} \leq 3.90$ nm.
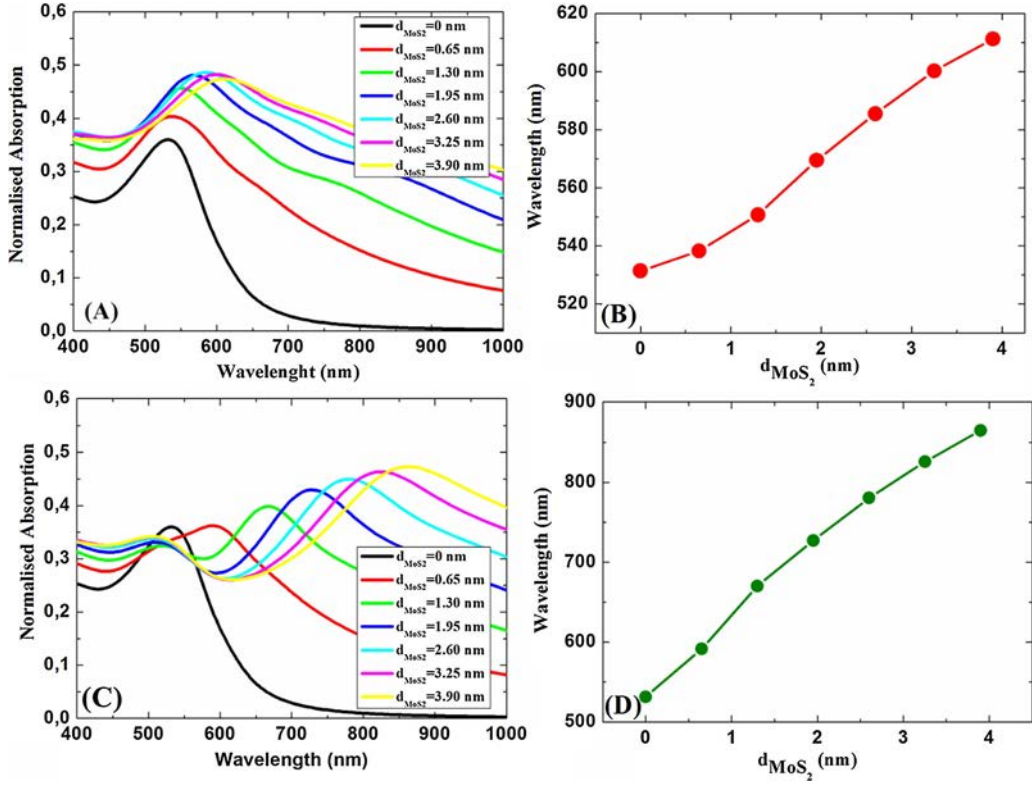
Fig. 2. (A) Variation in of absorption spectrum of the glass/Au NPs/MoS$_2$ interface (Fig. 1A) as a function of the thickness of MoS$_2$ (d_{MoS_2} = 0–3.9 nm) when immersed in water. (B) Evolution of the position of the LSPR band as a function of the thickness of the MoS$_2$ coating; (C) Variation in of absorption spectrum of a glass/MoS$_2$/Au NPs interface (Fig. 1B) as a function of the thickness of MoS$_2$ (d_{MoS_2} = 0–3.9 nm) when immersed in water; (D) Evolution of the position of the LSPR band as a function of the thickness of the MoS$_2$ underlying coating.

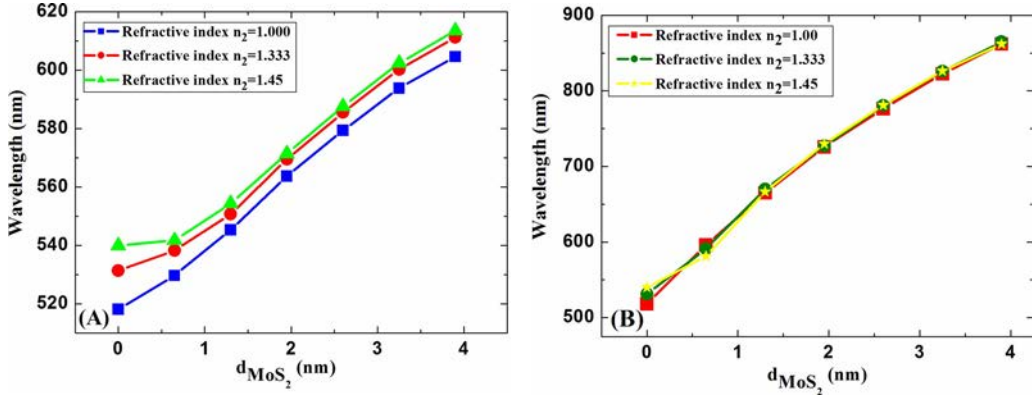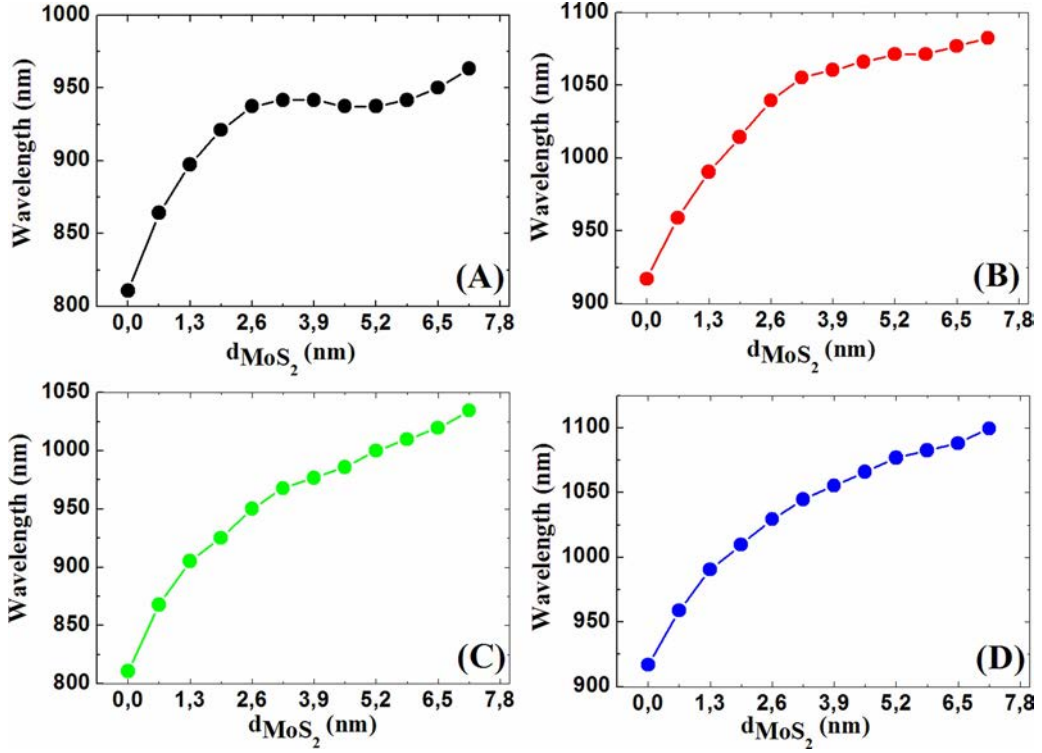**Fig. 3.** Evolution of λ_{max} with the thickness of the overcoat MoS$_2$, comparison upon change of the refractive index of the surrounding medium: (A) for structure "Fig. 1(A)", air (blue square), water (red circle) and SiO$_x$ (green triangle). (B) for structure "Fig. 1(B)", air (red square), water (olive circle) and SiO$_x$ (yellow star). The nanoparticles are characterized by l = 25 nm, h = 20 nm and a = 70 nm. The refractive index of the substrate on which they are deposited is n_1 = 1.45. (For interpretation of the references to color in this figure legend, the reader is referred to the web version of this article.)

In the purpose of comparing the absorption spectrum of results calculated with the model of L–D by the FEM method (for 0.65 nm ≤ d_{MoS_2} ≤ 3.90 nm thickness of MoS$_2$ layer) are structures that were studied in Fig. 2. Which shows the evolution of the normalized absorption resonance wavelength of the two structures according thick MoS$_2$, after the interaction of the studs with a light pulse incident [400–1000 nm]. The parameter values selected structures are: l = 25 nm, a = 70 nm and h = 20 nm. Giving the structure SiO$_x$/MoS$_2$/AuNPs/water a very significant growth of the resonance wavelength of 333.7 nm plasmon which passes from 531.35 nm to 865.05 nm (Fig. 2B). Relative that obtained in the structure SiO$_x$/AuNPs/MoS$_2$/water we see dramatic growth of the

Fig. 4. Evolution of λ_{max} with the thickness of the overcoat MoS$_2$ comparison of different refractive index of the medium surrounding structure (Fig. 1(A)), (A) air $n_2 = 1.000$ and (B) SiO$_x$ $n_2 = 1.45$. Comparison with the structure (Fig. 1(B)), (C) air $n_2 = 1.000$), and (D) and SiO$_x$ $n_2 = 1.45$. The nanoparticles are characterized by $l = 125$ nm, $h = 15$ nm and $a = 300$ nm. The refractive index of the substrate on which they are deposited is $n_1 = 1.45$.

resonance wavelength of the plasmon studs which pass 538.21–611.25 nm (Fig. 2D), with an offset of 73.04 nm to the red. The change in position of λ_{max}, shows a linear dependence as a function of the thickness of the surrounding environment. Fig. 3(B) shows the influence of the refractive index of the detection medium on the plasmon response of the system studied. Contrary to what has been observed in Fig. 3(A), λ_{max} presents a spectral shift to red when the nanoparticles are started to be covered for deferments n_2 media.

It was investigated by recording that the wavelength shifts when it is changed, in small proportions giving 518.13 nm for air, 531.35 nm for water and 539.96 nm for SiO$_x$ at d$_{MoS_2}$ = 0 nm, with the sensitivity of $S = 39.68$ nm/RIU, and 776.40 nm for air, 780.49 nm for water and 781.25 nm for SiO$_x$ at d$_{MoS_2}$ = 2.60 nm with the sensitivity $S = 12.28$ nm/RIU. It is found that the sensitivity, like the resonance wavelength, shows a weak oscillation when n_2 increases. The studied system thus has a non-zero sensitivity, but this is small and always less than the sensitivity of the nanoparticles covered by MoS$_2$, for the n_2 values to be considered. Indeed, for $n_2 = 1.000$, 1.333 and 1.45, Almost a small variation of the resonance wavelength is observed. Moreover, for the thickness of MoS$_2$ increases, the resonance wavelength is shifted towards the red as Fig. 3B. These behavioral differences are simply due to the way the refractive index (n_2) by the nanoparticles varies and geometrical parameters Au nanoparticles. Fig. 4, it is deduced that whatever the value of n_2, and for large geometrical parameters of the structure $l = 125$ nm $a = 300$ nm and $h = 15$ nm, the sensitivity and the resonance wavelength of the structures studied are presented extremely for the same thicknesses of d$_{MoS_2}$. Note also that the sensitivity and the resonance wavelength oscillate as a function of d$_{MoS_2}$. However, it is now known that the value of the refractive index of the detection medium (n_2) and the geometric characteristics of the nanoparticles have an impact on the displacement of LSPR and the sensitivity. Moreover, it can be deduced that the sensitivity is oscillated for two reasons. On the one hand, the fact of depositing the layer of MoS$_2$ under the nanoparticles is detrimental to the sensitivity, and causes a decrease in the latter for the thicknesses of d$_{MoS_2}$ (0.65–7.15 nm). On the other hand, the refractive index of the dielectric covering the nanoparticles (n_2) is lower than the refractive index of the medium which deposits the AuNPs ($n_1 = 1.45/n_{MoS_2} = 5.9 + 0.8\,i$), and the geometric parameters of system, that's what we can check in Fig. 4 and Table 2.

This variation in the effect of geometric parameters of gold nanoparticles leads to the increase of detection optic properties. Increasing the geometric parameters of the AuNPs first generates an increase in the wavelength of plasmon resonance. The increase in λ_{max} is consistent with the evolution of the electric field contact within the gold nanoparticles. These results are consistent with other reports in the literature showing long row detecting refractive index on the plasmonic nanostructures [46] have studied these effects, which show a linear dependence as a function of the refractive index of the surrounding medium.

The refractive index sensitivity, defined as the ratio of the variation of the position of the plasmon band during the variation of the

Table 2

Comparison of the evolution of sensitivity acquired theoretically for glass/AuNPs/MoS$_2$ and glass/MoS$_2$/AuNPs. The nanoparticles are characterized by $l = 125$ nm, $h = 15$ nm and $a = 300$ nm. The refractive index of the substrate on which they are deposited is $n_1 = 1.45$.

	MoS$_2$	Thickness (nm)	Sensitivity (nm/RIU)
Glass/AuNPs/MoS$_2$	0	–	236.04
	1	0.65	210.46
	2	1.30	206.95
	3	1.95	207.64
	4	2.60	226.90
	5	3.25	252.38
	6	3.90	264.23
	7	4.55	285.53
	8	5.20	297.62
	9	5.85	288.28
	10	6.50	281.55
	11	7.15	264.82
Glass/MoS$_2$/AuNPs	0	–	236.04
	1	0.65	202.52
	2	1.30	189.76
	3	1.95	187.79
	4	2.60	175.97
	5	3.25	171.19
	6	3.90	174.51
	7	4.55	177.94
	8	5.20	170.94
	9	5.85	161.91
	10	6.50	152.59
	11	7.15	144.43

refractive index (Eq. (2)) and determinable from the slop of a quasi-linear plot of λ_{max} vs. n_2 [47].

$$S = \frac{\Delta\lambda_{\max}}{\Delta n_2} \, (\text{nm RIU}^{-1})$$
(2)

Of both interfaces us shown in Table 2. Two circles used to determine the sensitivity for the same interface indexes in the $n_2 = 1.45$ material and air $n_2 = 1$ ($\Delta n_2 = 0.45$).

Fig. 4, shows the change of λ_{max} with the refractive index of different dielectrics used to put some dielectric layers (MoS$_2$) and gold nanostructures.

Several numerical simulations were done to find out how changing the sensitivity depend on the thickness of MoS$_2$ filed on nanoparticles (AuNPs/MoS$_2$) or between the substrate and the nanoparticles (MoS$_2$/AuNPs).

These results are in agreement with other reports, in the field of study, showing long rank refractive index of detection of plasmonic nanostructures [46] Table 1, exposes this evolution of sensitivity according to the layer thickness of MoS$_2$.

We have initially determined the sensitivity of the system described in Fig. 1, without the thickness of MoS$_2$ (d$_{MoS_2}$ = 0 nm) above or below the gold nanoparticles. The wavelength of resonance of such a system is $\lambda_{max} = 810.81$ nm for $n_2 = 1.000$ and $\lambda_{max} = 917.03$ nm for $n_2 = 1.45$, we find $S = 236.04$ nm/RIU.
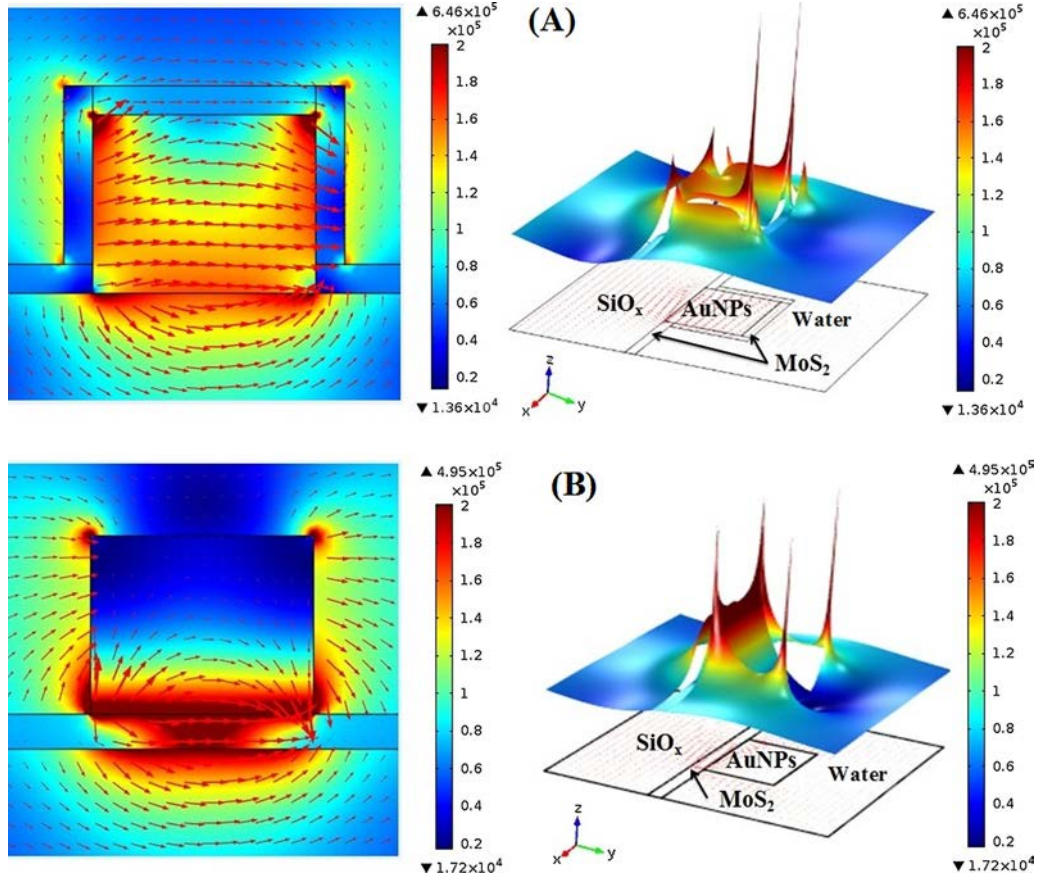
On the other hand, for (d$_{MoS_2}$), either when the nanoparticles are covered by different MoS$_2$ slips or when the nanoparticles are covered with 8 layers of MoS$_2$ (d$_{MoS_2}$ = 5.20 nm), the resonance wavelength is $\lambda_{max} = 937.5$ nm for $n_2 = 1.000$ and $\lambda_{max} = 1071.43$ nm for $n_2 = 1.45$, which corresponds to a sensitivity of $S = 297.62$ nm/RIU.

For a thickness of MoS$_2$ (from 0.65 to 7.15 nm) we vary in sensitivity by changing the thickness of MoS$_2$. We find that the sensitivity is proportional to the thickness of MoS$_2$. First of all, there has been an increase in sensitivity (glass/AuNPs/MoS$_2$) for thicknesses of MoS$_2$ between 1.95 and 5.20 nm. Indeed, $S = 206.95$ nm/RIU for 2 layers (1.30 nm) and $S = 297.62$ nm/RIU to 5.20 nm, after we noticed a decrease in sensitivity from thickness 9 layers (5.85 nm).

Indeed, the sensitivity that corresponds to the structure (Fig. 1B) is decreasing when the thickness of the layer of MoS$_2$ diminished, $S = 202.52$ nm/RIU for d$_{MoS_2}$ = 0.65 nm at $S = 144.43$ nm/RIU for d$_{MoS_2}$ = 7.15 nm [20,22,48,49]. The enhancement of sensitivity for the AuNPs/MoS$_2$ based LSPR biosensor is calculated to have more than 26% of when compared the sensors LSPR conventional without the layer of MoS$_2$, with the same parameters of AuNPs. These characteristics should make these biosensors a preferred choice for bio-detection applications, compared to other contemporary biosensors.

3.2. Influence of dielectric MoS$_2$ on the distribution of electric field

The sensitivity of the interface can be understood from the electrical field maps in Fig. 5 shows the distribution of the electric field to the resonance near nanoparticles. It can be seen by comparing Fig. 5(A) that when the nanoparticles (Au NPs) are covered with MoS$_2$ a substantial part of the field is found inside of the latter. In the case of MoS$_2$ coated glass Fig. 5(B) that when the nanoparticles covered with a non-absorbing dielectric (water) the field spreads out more and more deeply into the substrate as that its refractive

Fig. 5. Electric field maps on (A) glass/AuNPs/MoS$_2$ for d$_{MoS_2}$ = 2.60 nm under monochromatic incident radiation at 585 nm; (B) glass/MoS$_2$/AuNPs for d$_{MoS_2}$ = 3.90 nm under monochromatic incident radiation at 865 nm.

index increases (MoS$_2$).

Maps of calculated electric field Fig. 5(A) to the resonance wavelength plasmon λ_{max} = 585.48 nm for d$_{MoS_2}$ = 2.60 nm show a strong improvement of the field located on the four corners of the nanoparticles within the confined field. The corners of AuNPs with strong localization at the upper corners of AuNPs compared to the structure of Fig. 5(B) calculated at the resonant wavelength plasmon λ_{max} = 865.05 nm d$_{MoS_2}$ = 3.90 nm a strong localization is observed at the upper corners and at the lower surface of the AuNPs in contact with the layer of MoS$_2$ [50–52]. It is thus seen in Fig. 5(B), that in the MoS$_2$ nanoparticles, the present two hotspots electric field at the upper corners of AuNPs and the surface in contact with the substrate. In addition, Fig. 5(A) shows that the nanoparticles coated with 2.60 nm of MoS$_2$ have hot spots in each of their corners, and the two hot spots in contact with the substrate have spread spatially. Furthermore, the addition of MoS$_2$ led to an increase of the amplitude of the electric field in both sides of AuNPs in contact with this medium recouvrement.

Fig. 6 shows the change in the resonance wavelength depending on the thickness of d$_{MoS_2}$ MoS$_2$ layers deposited below the gold nanoparticles to study the structure SiO$_x$/MoS$_2$/AuNPs/water, The effect of the allowance index of dielectric substrate.
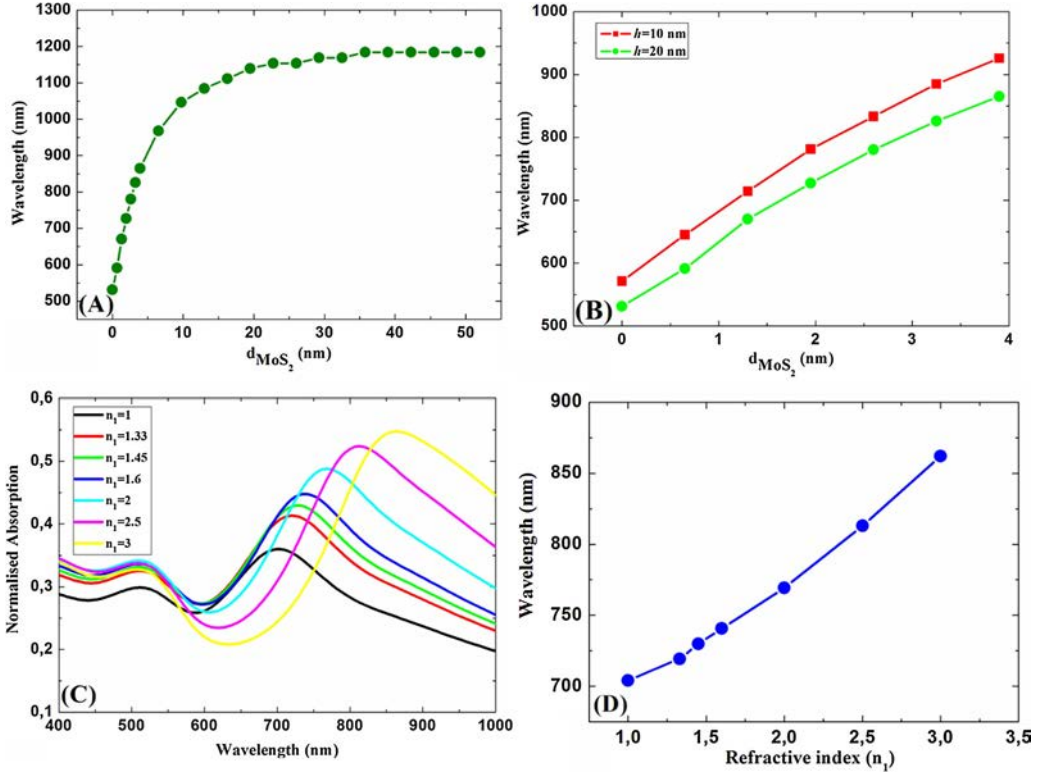
Fig. 6(A) shows the change in resonance wavelength as a function of the thickness d$_{MoS_2}$, studied for the structure SiO$_x$/MoS$_2$/AuNPs/water. It is found that the λ_{max} of shift for the same detection medium is different d$_{MoS_2}$ value from 0 to 50 nm. Fig. 6(A) shows the influence of the thickness of the dielectric layer on the plasmonic response of the system studied SiO$_x$/MoS$_2$/AuNPs/water. Indeed, the resonant wavelength is not shifted towards the red but remains constant. It is recalled that the refractive index of the substrate is n_1 = 1.45 (SiO$_x$), and which covers the nanoparticles with a dielectric having a refractive index n_2 = 1 (water). For the variation of the thickness of MoS$_2$ from 0 to 19.25 nm resonance wavelength plasmon red-shifted from 531.35 nm to 1168.83 nm. Then from d$_{MoS_2}$ = 29.25 nm, there is almost no variation observed in the resonant wavelength LSPR.

Fig. 6(B) shows that the resonant wavelength plasmon increases when the height decreases, λ_{max} = 531.3 nm for h = 20 nm and λ_{max} = 571.4 nm for h = 10 nm to d$_{MoS_2}$ = 0 nm, and λ_{max} = 865 nm for h = 20 nm and λ_{max} = 926 nm for h = 10 nm to six layers of MoS$_2$ d$_{MoS_2}$ = 3.90 nm. This red shift of LSPR when the height (h) decreases when d$_{MoS_2}$ remains constant increases, is varied from 40 to 60 nm.

This is what highlights Fig. 6. We can see the evolution of the position of resonance, when the dielectric substrate of refractive index changes to the value of d$_{MoS_2}$ = 1.95 nm distinct.

As before, we mapped the absorption spectra of the studied MoS$_2$/AuNPs system for d$_{MoS_2}$ = 1.95 nm (3 layers of MoS$_2$), in order

Fig. 6. (A) Evolution of LSPR peak with change in thickness of the layer of MoS_2 (d_{MoS_2}) of the structure (Fig. 1B) $SiO_x/MoS_2/AuNPs/water$, for $a = 70$ nm, $l = 25$ nm and $h = 20$ nm. (B) Evolution of λ_{max} with the thickness of the overlay MoS_2 ($SiO_x/MoS_2/AuNPs/water$) to compare two values of the height (h) of gold nanoparticles ($h = 10$ nm red square) and ($h = 20$ nm green circle), the other parameters are $a = 70$ nm, $l = 25$ nm. (C) Absorption spectrum corresponding to the structure substrate/MoS_2/AuNPs/water for defeated refractive index of the substrate. (D) Change in the resonant wavelength in plasmon function of refractive index of the dielectric substrate. The geometric parameters of the gold nanoparticles are: $l = 25$ nm, $h = 20$ nm, $a = 70$ nm and $d_{MoS_2} = 1.95$ nm. (For interpretation of the references to color in this figure legend, the reader is referred to the web version of this article.)

to analyze the influence of n_1 on the plasmonic response of the nanoparticles (see Fig. 6(C)). It appears, similar to what was found for Fig. 2(C), that the growth of the amplitude of absorption spectra when n_1 increases, coincides with the appearance of new modes of plasmonic resonance in addition to the main mode [21,43]. This is what highlights Fig. 6. We can see the evolution of the position of resonance, when the dielectric substrate of refractive index changes to the value of $d_{MoS_2} = 1.95$ nm distinct. In Fig. 6(C), one can verify that λ_{max} is red-shifted when the substrate refractive index increases, it therefore becomes independent from you the value of the refractive index of the substrate.

Moreover, Fig. 6(D) depicts the change in the localised surface plasmonic resonance (λ_{max}) with the substrate refractive index, there is a very significant linear increase $\lambda_{max} = 704.23$ nm to $\lambda_{max} = 862$ nm, with an amplitude of 0.36–0.55 calculated for the substrate refractive index increases from $n_1 = 1$ to $n_1 = 3$. This observation is important to search for a plasmonic sensor to optimal properties.

4. Conclusion

We have theoretically studied the optical properties of the influence of the dielectric film with MoS_2 nanoparticles of gold structure on plasmonic properties and sensitivity. The Lorentz–Drude model was used to calculate the optical signal of localized surface plasmon resonance (LSPR) gold nanostructures $SiO_x/AuNPs/MoS_2/water$ and $SiO_x/MoS_2/AuNPs/water$; this study provides a better understanding resonance coupled to systems based on gold nanoparticles and MoS_2 layers. Due to this research put into the development of the surface plasmon functionalization of hybrid interfaces applications. Developing several sensing components, the offset to the wavelength of red, localization of the electric field and sensitivity of the interface hybrid of the LSPR depends on thickness of the MoS_2 layer. A general conclusion can be drawn that the interest in these multilayer interfaces is the possibility of sensitive long detection range with important implications for biological detection studies.

References

[1] E.M. Larsson, J. Alegret, M. Kll, D.S. Sutherland, Sensing characteristics of NIR localized surface plasmon resonances in gold nanorings for application as

ultrasensitive biosensors, Nano Lett. 7 (2007) 1256–1263.

[2] L.B. Scaffardi, J.O. Tocho, Size dependence of refractive index of gold nanoparticles, Nanotechnology 17 (2006) 1309–1315.

[3] P. Hanarp, M. Kll, D.S. Sutherland, Optical properties of short range ordered arrays of nanometer gold disks prepared by colloidal lithography, J. Phys. Chem. B 107 (2003) 5768–5772.

[4] H. Chen, X. Kou, Z. Yang, W. Ni, J. Wang, Shape- and size-dependent refractive index sensitivity of gold nanoparticles, Langmuir 24 (2008) 5233–5237.

[5] R. Bukasov, J.S. Shumaker-Parry, Highly tunable infrared extinction properties of gold nanocrescents, Nano Lett. 7 (2007) 1113–1118.

[6] J. Aizpurua, P. Hanarp, D.S. Sutherland, M. Kll, G.W. Bryant, F.J. Garcia de Abajo, Optical properties of gold nanorings, Phys. Rev. Lett. 90 (2003) 057401.

[7] C. Langhammer, M. Schwind, B. Kasemo, I. Zoric, Localized surface plasmon resonances in aluminum nanodisks, Nano Lett. 8 (2008) 1461–1471.

[8] J. Ye, P. Van Dorpe, L. Lagae, G. Maes, G. Borghs, Observation of plasmonic dipolar anti-bonding mode in silver nanoring structures, Nanotechnology 20 (2009) 465203.

[9] I. Zoric, M. Zch, B. Kasemo, C. Langhammer, Gold, platinum, and aluminum nanodisks plasmons: material independence, subradiance, and damping mechanisms, ACS Nano 5 (2011) 2535–2546.

[10] A. Pinchuk, A. Hilger, G. Von Plessen, U. Kreibig, Substrate effect on the optical response of silver nanoparticles, Nanotechnology 15 (2004) 1890–1896.

[11] M. Valamanesh, Y. Borensztein, C. Langlois, E. Lacaze, Substrate effect on the plasmon resonance of supported flat silver nanoparticles, J. Phys. Chem. C 115 (2011) 2914–2922.

[12] A.O. Pinchuk, G.C. Schatz, Nanoparticle optical properties: far- and near-field electrodynamic coupling in a chain of silver spherical nanoparticles, Mater. Sci. Eng. B 149 (2008) 251–258.

[13] A.M. Funston, C. Novo, T.J. Davis, P. Mulvaney, Plasmon coupling of gold nanorods at short distances and in different geometries, Nano Lett. 9 (2009) 1651–1658.

[14] W. Rechberger, A. Hohenau, A. Leitner, J.R. Krenn, B. Lamprecht, F.R. Aussenegg, Optical properties of two interacting gold nanoparticles, Opt. Commun. 220 (2003) 137–141.

[15] E. Galopin, A. Noual, J.N. Jonsson, J.N. Martin, A. Akjouj, Y. Pennec, B.D. Rouhani, R. Boukherroub, S. Szunerits, Short- and long-range sensing using plasmonic nanostructures: experimental and theoretical studies, J. Phys. Chem. C 113 (2009) 15921–15927.

[16] H. Zhang, Y. Ma, Y. Wan, X. Rong, Z. Xie, W. Wang, L. Dai, Measuring the refractive index of highly crystalline monolayer MoS_2 with high confidence, Sci. Rep. 5 (2015) 8440.

[17] S. Zenga, S. Hub, J. Xiac, T. Anderson, X.Q. Dinh, X.-M. Meng, P. Coqueta, K.T. Yonga, Graphene-MoS_2 hybrid nanostructures enhanced surface plasmon resonance biosensors, Sens. Actuators B 10 (2014).

[18] A.K. Mishra, S.K. Mishra, MgF_2 prism/rhodium/graphene: efficient refractive index sensing structure in optical domain, J. Phys. Condens. Matter 29 (2017) 145001.

[19] N. Sharma, A. Joy, A.K. Mishra, R.K. Verma, Fuchs Sondheimer–Drude Lorentz model and Drude model in the study of SPR based optical sensors: a theoretical study, Opt. Commun. 357 (2015) 120–126.

[20] A.K. Mishra, S.K. Mishra, R.K. Verma, Graphene and beyond graphene MoS_2: a new window in surface-plasmon-resonance-based fiber optic sensing, J. Phys. Chem. C 120 (2016) 2893–2900.

[21] L. Wu, H.S. Chu, W.S. Koh, E.P. Li, Highly sensitive graphene biosensors based on surface plasmon resonance, Opt. Express 18 (2010) 14395–21440.

[22] C. Lertvachirapaiboon, A. Baba, S. Ekgasit, C. Thammacharoen, K. Shinbo, K. Kato, F. Kaneko, Gold nanoparticles synthesis used for sensor applications, IEEE Conf. Proc. ISEIM (2014), http://dx.doi.org/10.1109/ISEIM.2011.6826352.

[23] K.M. Mayer, J.H. Hafner, Localized surface plasmon resonance sensors, Chem. Rev. 111 (2011) 3828–3857.

[24] S. Szunerits, R. Boukherroub, Sensing using localised surface plasmon resonance sensors, Chem. Commun. 48 (2012) 8999–9010.

[25] L. Touahir, E. Galopin, R. Boukherroub, A.C. Gouget-Laemmel, J.N. Chazalviel, F. Ozanam, O. Saison, A. Akjouj, Y. Pennec, B. Djafari-Rouhani, Plasmonic properties of silver nanostructures coated with an amorphous silicon-carbon alloy and their applications for sensitive sensing of DNA hybridization, Analyst 136 (2011) 1859.

[26] M.D. Malinsky, K.L. Kelly, G.C. Schatz, R.P. Van Duyne, Chain length dependence and sensing capabilities of the localized surface plasmon resonance of silver nanoparticles chemically modified with alkanethiol self-assembled monolayers, J. Am. Chem. Soc. 123 (2001) 1471.

[27] A.J. Haes, S. Zou, G.C. Schatz, R.P.J. Van Duyne, Nanoscale optical biosensor: short range distance dependence of the localized surface plasmon resonance of noble metal nanoparticles, J. Phys. Chem. B 108 (2004) 6961–6968.

[28] H. Xu, M. Kll, Modeling the optical response of nanoparticle-based surface plasmon resonance sensors, Sens. Actuators B 87 (2002) 244.

[29] A.J. Haes, W.P. Hall, L. Chang, W.L. Klein, R.P. Van Duyne, Nanoscale localized surface plasmon resonance biosensors, Nano Lett. 4 (2004) 1029.

[30] W.A. Murray, J.R. Suckling, W.L. Barnes, Overlayers on silver nanotriangles: field confinement and spectral position of localized surface plasmon resonances, Nano Lett. 6 (2006) 1772.

[31] T. Rindzevicius, Y. Alaverdyan, M. Kll, W.A. Murray, W.L. Barnes, Long-range refractive index sensing using plasmonic nanostructures, J. Phys. Chem. C 111 (2007) 11806.

[32] A. Gupta, G. Chen, P. Joshi, S. Tadigadapa, P.C. Eklund, Raman scattering from high-frequency phonons in supported n-graphene layer films, Nano Lett. 6 (2006) 2667–2673.

[33] D.Y. Lei, A.I. Fernandez-Domanguez, Y. Sonnefraud, K. Appavoo, R.F. Haglund, J.B. Pendry, S.A. Maier, Revealing plasmonic gap modes in particle-on-film systems using dark-field spectroscopy, ACS Nano. 6 (2012) 1380–1386.

[34] A. Noual, Y. Pennec, A. Akjouj, B. Djafari-Rouhani, L. Dobrzynski, Nanoscale plasmon waveguide including cavity resonator, J. Phys. Condens. Matter 21 (2009) 375301.

[35] M.W. Knight, N.J. Halas, Nanoshells to nanoeggs to nanocups: optical properties of reduced symmetry core–shell nanoparticles beyond the quasistatic limit, New J. Phys. 10 (2008) 105006.

[36] J.M. Jin, The Finite Element Method in Electromagnetics, Livre, 1993.

[37] Y. Zhan, D.Y. Lei, X. Li, S.A. Maier, Plasmonic Fano resonances in nanohole quadrumers for ultra-sensitive refractive index sensing, Nanoscale (2014), http://dx.doi.org/10.1039/C3NR06024A.

[38] A.D. Rakic, A.B. Djuristic, J.M. Elazar, M.L. Majewski, Analysis of optical channel cross talk for free-space optical interconnects in the presence of higher-order transverse modes, Appl. Opt. 37 (1998) 5271–5283.

[39] C.J. Powell, Analysis of optical- and inelastic-electron-scattering data. II. Application to Al, J. Opt. Soc. Am. 60 (1970) 78–93.

[40] A. Castellanos-Gomez, N. Agrait, G. Rubio-Bollinger, Optical identification of atomically thin dichalcogenide crystals, Appl. Phys. Lett. 96 (2010) 213116.

[41] T. Rindzevicius, Y. Alaverdyan, M. Kall, W.A. Murray, W.L. Barnes, Long-range refractive index sensing using plasmonic nanostructures, J. Phys. Chem. C 111 (2007) 11806–11810.

[42] B. Mukherjee, F. Tseng, D. Gunlycke, K.K. Amara, G. Eda, E. Simsek, Complex electrical permittivity of the monolayer molybdenum disulfide (MoS_2) in near UV and visible, Opt. Mater. Express 5 (2) (2015) 447–455.

[43] O. Saison-Francioso, G. Lvque, A. Akjouj, Y. Pennec, B. Djafari-Rouhani, S. Szunerits, R. Boukherroub, Plasmonic nanoparticles array for high-sensitivity sensing: a theoretical investigation, J. Phys. Chem. C 116 (33) (2012) 17819–17827.

[44] A.K. Mishra, S.K. Mishra, Infrared SPR sensitivity enhancement using ITO/TiO_2/silicon overlays, Europhys. Lett. 112 (2015) 10001.

[45] A.K. Mishra, S.K. Mishra, R.K. Verma, An SPR-based sensor with an extremely large dynamic range of refractive index measurements in the visible region, J. Phys. D: Appl. Phys. 48 (2015) 435502.

[46] E. Galopin, J. Niedzioka-Jonsson, A. Akjouj, Y. Pennec, B. Djafari-Rouhani, A. Noual, R. Boukherroub, S. Szunerits, Sensitivity of plasmonic nanostructures coated with thin oxide films for refractive index sensing: experimental and theoretical investigations, J. Phys. Chem. C 114 (2010) 11769–11775.

[47] A.J. Haes, R.P. Van Duyne, A nanoscale optical biosensor: sensitivity and selectivity of an approach based on the localized surface plasmon resonance spectroscopy of triangular silver nanoparticles, J. Am. Chem. Soc. 124 (2002) 105–196.

[48] A.K. Mishra, S.K. Mishra, Gas sensing in Kretschmann configuration utilizing bi-metallic layer of Rhodium-Silver in visible region, Sens. Actuators B: Chem. 237 (2016) 969–973.

[49] A.K. Mishra, S.K. Mishra, R.K. Verma, Doped single-wall carbon nanotubes in propagating surface plasmon resonance based fiber optic refractive index sensing, Plasmonique 12 (2017) 1657–1663.

[50] J. Cao, J. Wang, G. Yang, Y. Lu, R. Sun, P. Yan, S. Gao, Enhancement of broad-band light absorption in monolayer MoS_2 using Ag grating hybrid with distributed Bragg reflector, Superlattices Microstruct. 110 (2017) 26–30.

[51] P. Viste, J. Plain, R. Jaffiol, A. Vial, P.-M. Adam, P. Royer, Enhancement and quenching regimes in metal-semiconductor hybrid optical nanosources, ACS Nano 4 (2010) 759–764.

[52] T. Hutter, S.R. Elliott, S. Mahajan, Interaction of metallic nanoparticles with dielectric substrates: effect of optical constants, Nanotechnology 24 (2013) 035201.